View metadata, citation and similar papers at core.ac.uk
brought to you by CORE
provided by University of Essex Research Repository

Dual-drive $LiNbO_3$ interferometric Mach-Zehnder architecture with extended linear regime for high peak-to-average OFDM-based communication systems

Maria Morant,[1,*] Roberto Llorente,[1] Jerome Hauden,[2] Terence Quinlan,[3] Alexandre Mottet,[2] and Stuart Walker[3]

[1]*Nanophotonics Technology Centre, Universidad Politécnica de Valencia, Camino de Vera s/n, 46022 Valencia, Spain*
[2]*Photline Technologies, 16 rue Jouchoux, 25000 Besançon, France*
[3]*School of Computer Science and Electronic Engineering, University of Essex, Wivenhoe Park, Colchester, CO4 3SQ, UK*
**mmorant@ntc.upv.es*

Abstract: A dual-drive $LiNbO_3$ architecture modulator with chirp management is proposed and developed offering SFDR > 25 dB in a 1.4 V bias excursion compared to only 0.5 V bias excursion in a conventional Mach-Zehnder electro-optical modulator (MZ-EOM). The architecture effectively extends the linear regime and enables the optical transmission of wireless systems employing orthogonal division multiplexing (OFDM) modulation such as ultra-wide band (UWB) which require high linearity over a broad frequency range due to their high peak-to-average power ratio (PARP). Radio-over-fiber UWB transmission in a passive optical network is experimentally demonstrated employing this technique, exhibiting an enhancement of 2.2 dB in EVM after 57 km SSMF when the dual-drive developed modulator is employed.

©2011 Optical Society of America

OCIS codes: (130.4110) Modulators; (060.4510) Optical communications.

References and links

1. M. Morant, T. Quinlan, R. Llorente, and S. Walker, "Full standard triple-play bi-directional and full-duplex CWDM transmission in passive optical networks," in *Proceedings of OFC/NFOEC 2011*, OWB3, (2011).
2. J. Pham and A. C. Carusone, "A time-interleaved 16-DAC architecture clocked at the Nyquist rate," IEEE Trans. Circuits Syst. II **55**(9), 858–862 (2008).
3. Y. H. You, I. T. Hwang, C. K. Song, and H. K. Song, "PAPR analysis for multi-band OFDM signals," Electron. Lett. **41**(5), 261–262 (2005).
4. T. Alves, M. Morant, A. Cartaxo, and R. Llorente, "Performance comparison of OFDM-UWB radio-signals distribution in long-reach PONs using Mach-Zehnder and linearized modulators," IEEE J. Sel. Areas Comm. **29**(6), 1311–1320 (2011).
5. S. K. Kim, J. Lee, and J. Jeong, "Transmission performance of 10-Gb/s optical duobinary transmission systems considering adjustable chirp of nonideal $LiNbO_3$ Mach–Zehnder modulators due to applied voltage ratio and filter bandwidth," J. Lightwave Technol. **19**(4), 465–470 (2001).
6. ECMA-368: "High rate ultra-wideband PHY and MAC Standard," ECMA International Standard (Dec. 2007).

1. Introduction

Radio-over-fiber transmission of several wireless services in coexistence through the same optical network requires electro-optic modulators (EOM) with excellent dynamic range and an extensive linear regime [1]. Transmitter digital-to-analog converters for radio systems employing orthogonal division multiplexing (OFDM) modulation such as ultra-wide band (UWB) require a linearity of at least 25 dB [2]. Multi carrier signals with large number of sub-channels like multi-band OFDM-UWB signals have large peak-to-average power ratio

#155666 - $15.00 USD
Received 3 Oct 2011; accepted 9 Oct 2011; published 22 Nov 2011
(C) 2011 OSA

(PAPR) which joint with the high bandwidth of each UWB channel (528 MHz) is the main limitation of intensity-modulation systems [3]. In this work, a dual drive (DD) Mach-Zehnder (MZ) architecture with enhanced linearity and chirp controlled modulation scheme was designed, characterized and applied to radio-over-fiber transmission of high PAPR signals.

Also, radio-over-fiber systems can take advantage of this chirp management as the produced chirp combined with the dispersion the transmission □ber in optical access networks can compensate the effects of the optical transmission and, as a result, improve the overall performance of the system [4]. Chirp control measurements obtained with the developed dual-drive modulator are reported in Section 3. In Section 4 the performance comparison with a conventional Mach-Zehnder modulator is examined. Finally in Section 5, the DD-MZ was assessed in a UWB-over-fiber transmission of high PAPR signals.

2. Modulator design and characterization

The dual-drive modulator architecture is described in Fig. 1(a). It has one broadband RF-electrode per optical arm of the optical interferometer. This DD-MZ requires two electrical signals, each driving the modulator at half the voltage of a single-drive device. Normal operation consists of applying half of the required electrical amplitude on each RF port, RF + and RF-, with a π phase shift between them: + V/2, -V/2. By design, both electrodes are synchronized so as to modulate the optical field at the same time and with the same group delays. In standard usage, both modulating signal voltages are equal so as to provide intensity modulation. Naturally, one can modify the amplitude (and phase) of the modulating signals for specific applications. In this way, the electro-optical field overlap in each arm of the interferometer can be varied significantly if required, leading to the presence or the absence of residual phase modulation and hence frequency chirp control (sign and amplitude). This process can be adjusted so as to mitigate or enhance the effect of fiber dispersion. Moreover, when applying an appropriate phase-delay between input signals (typically ± π/2) it is possible to suppress harmonics in the modulated optical spectrum (typically first order modulation harmonic) and a single-side band (SSB) modulation spectrum can be obtained.

Figure 1(b) show the eye diagrams measured at data rates of 10 and 20 Gbps when the DD-MZ modulator is driven by two amplifiers delivering half of the voltages ($V_\pi/2$) in opposite of phase. The low RMS time jitters (1.37 ps @ 20Gbps) show the very good synchronization of all the RF-lines. The packaged device was characterized in back-back configuration (detection just after the modulator). Figure 1(a) shows the electrical back-reflection in S_{11} and S_{21} and the bandwidths that arrive up to 10 GHz @ –3 dB. The third order intersection point (IP3), indicating the spurious free dynamic range (SFDR) was characterized for each RF-port. Figure 2 shows the characterization of the fabricated DD-MZ. The IP3 related to the input was measured to be at least of 36 dBm @ 5 GHz as shown in Fig. 2(b). For a noise floor of –120 dBm, the resulting SFDR is in the range of 60 dB.

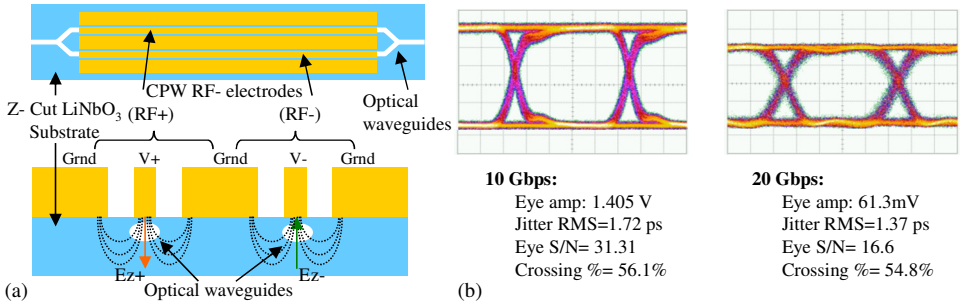

Fig. 1. (a) Scheme of the designed dual drive modulator chip in top view and cross section. (b) NRZ output eye diagrams for measured for 10 Gbps and 20 Gbps.

#155666 - $15.00 USD
Received 3 Oct 2011; accepted 9 Oct 2011; published 22 Nov 2011
(C) 2011 OSA

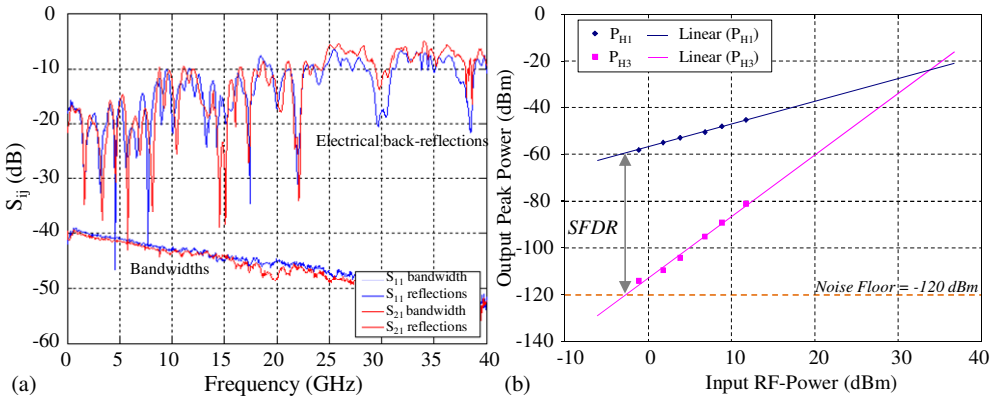

Fig. 2. (a) Bandwidths (lower traces) and electric back-reflections at the inputs for both RF-lines measured with the packaged DD-MZ modulators; (b) IP3 measurements on DD-MZ RF + at 5GHz.

3. Chirp measurement by frequency discrimination

Among different available techniques, the chirp produced by the EO-modulation was measured here by frequency discrimination [5] using the experimental setup shown in Fig. 3:

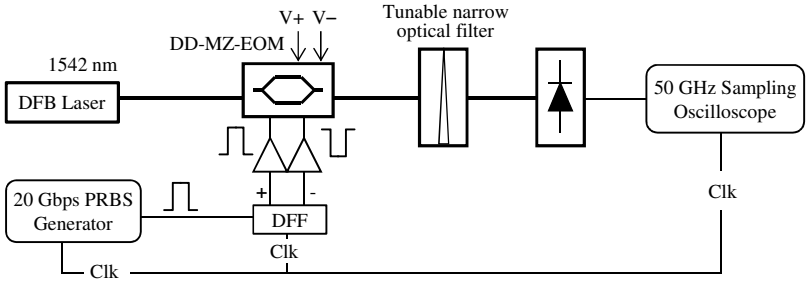

Fig. 3. Experimental set up for frequency chirp control and measurement.

The instantaneous pulsation in the presence of chirp, i.e phase modulation, is given at the output of a Mach-Zehnder Interferometer modulator by:

$$\omega(t) = \omega - \beta\kappa \frac{\partial V(t)}{\partial t} \quad \text{with} \quad \kappa = \frac{\pi}{2\eta_0 V_\pi} \tag{1}$$

where V_π is the half-wave voltage of the modulator; η_0 the mean EO overlap in both arm of the interferometer; and β the overlap discrepancy between them, source of the frequency chirp.

Considering a modulation Gaussian-like pulse $V(t)$ as:

$$V(t) = V_O \exp\left(-\frac{t^2}{\tau^2}\right) \tag{2}$$

The first derivative in function of time can be expressed as:

$$\frac{\partial V(t)}{\partial t} = -\frac{2t}{\tau^2} V_O \exp\left(-\frac{t^2}{\tau^2}\right) \tag{3}$$

#155666 - $15.00 USD
Received 3 Oct 2011; accepted 9 Oct 2011; published 22 Nov 2011
(C) 2011 OSA

According to Eq. (1), the instantaneous pulsation becomes:

$$\omega(t) = \omega + \beta\kappa \frac{2t}{\tau^2} \mathrm{V_O} \exp\left(-\frac{t^2}{\tau^2}\right) \tag{4}$$

When applying a pulse voltage of amplitude V_π, the instantaneous frequency turns into:

$$f(t) = \frac{\alpha}{4} \frac{2t}{\tau^2} \exp\left(-\frac{t^2}{\tau^2}\right) \tag{5}$$

with α the chirp parameter. Cancelling the first derivative of $f(t)$ we obtain the maximum frequency excursion occurs at $t_0 = \tau/\sqrt{2}$ and can be expressed as:

$$f_0 = \frac{\alpha}{2\sqrt{2}\tau} e^{-1/2} \tag{6}$$

At the output of the modulator, the narrow tunable optical filter is used as a frequency discrimination demodulator. It converts the residual phase modulation produced by the modulator (chirp) into intensity modulation, and adds it to the regular intensity modulation. Assuming it exhibits a symmetric transmission spectrum with a width ΔF, by recording two consecutive intensity modulations, one carried out on the positive slope (P^+) and the other on negative slope of the filter (P^-) one can deduce the frequency deviation as:

$$f - f_0 = \frac{\mathrm{P^+} - \mathrm{P^-}}{2\mathrm{P_0} e^{-1/2}} \frac{\Delta F}{\sqrt{2}} \tag{7}$$

where f_0 and P_0 are the central frequency and the maximum transmission optical power detected after the filter, respectively. From Eqs. (6) and (7) the chirp parameter α can be deduced.

In practice, as can be observed in Fig. 3, the DD-MZ is driven by two identical RF-amplifiers fed with a D-flip flop (DFF). Basically, the DFF makes a logic "AND" between the signal (square) from a PRBS generator and a clock signal. Both complementary outputs (+ and –) are connected to the amplifiers so as to get two amplified signals with a π-phase shift in between them. The modulator was fed with a series of short pulses, generating a relatively large spectrum. Due to non-infinite EO-bandwidths, we consider that the front and end edges of the pulses exhibit a Gaussian shape where the rising and falling times are equivalent to the τ parameter defined before.

Initially, the filter was centered on the optical carrier and then on the 3 dB left and right part of the optical spectrum. The output temporal signals were recorded as shown in Fig. 4(top) for signals at 20 Gbps. Numerically, the time responses are subtracted giving access to the frequency excursion, thus to the residual phase modulation, and then to the chirp parameter. Knowing the shape and the width of the optical filter one can isolate the resulting phase modulation. The sign is discriminated looking at the sign of the frequency amplitude.

#155666 - $15.00 USD Received 3 Oct 2011; accepted 9 Oct 2011; published 22 Nov 2011
(C) 2011 OSA

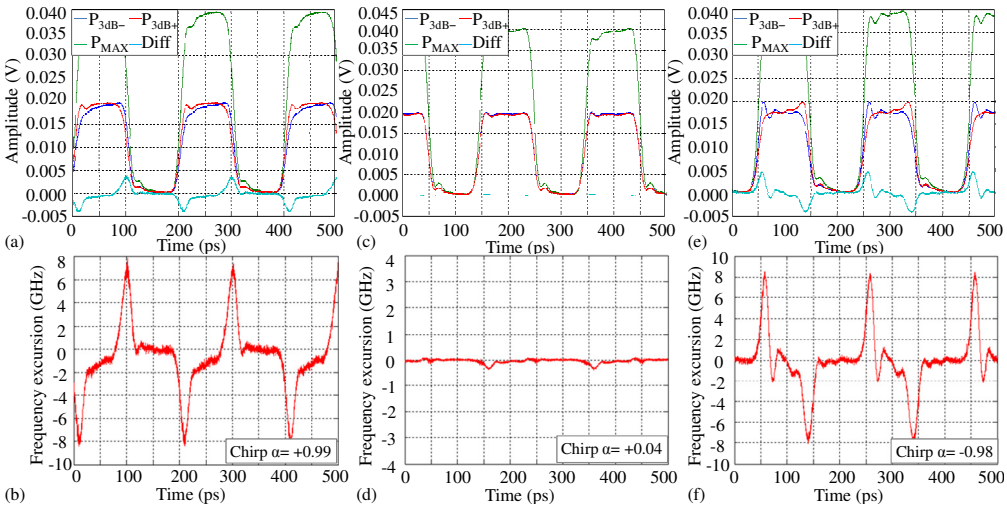

Fig. 4. 20 Gbps output temporally responses with three positions of the optical filter (top) and corresponding frequency excursion (bottom) for: (a-b) V + = Vπ, V- = 0, (c-d) V + = Vπ/2, V- = -Vπ/2, and (e-f) V + = 0, V- = Vπ.

First, the DD-modulator is exited at both RF-inputs with V + = V_π and V- = 0. In Fig. 4(a) we can note the spikes at the beginning and the end of each pulse due to non-zero frequency chirp. In Fig. 4(b) the chirp is estimated to be α = + 0.99, very close to 100%.

In the second case, the modulator is fed with two properly adjusted electric signals in phase opposition: V + = V_π/2 V- = -V_π/2. In Fig. 4(c) and 4(d) it can be observed that the difference is almost null even at the front and the end of the pulses. The frequency excursion illustrates an almost-zero chirp operation ($4 \cdot 10^{-2}$).

Finally, the third configuration is symmetric to the first case, V + = 0 and V- = V_π which temporal traces and obtained frequency excursion are shown in Fig. 4(e) and 4(f). As in the first case, spikes at the edge of the pulses are typical from frequency chirp. Note that in that case the spikes are in the opposite way compared to the first case: positive at the beginning, negative at the end. The chirp is negative and measured to be α = –0.98.

From these results we can confirm that using the DD-MZ the frequency chirp induced by the modulator can be tuned to any value between +/–100% by adjusting the balancing of the input voltages.

4. Performance comparison of the developed Dual-Drive with conventional modulators

The two-tone performance of the DD-MZ-EOM was evaluated and compared with a conventional single MZ-EOM (Covega LN-058) by considering two sinusoidal signals with frequencies of 4 GHz and 4.7 GHz. The optical link under study is depicted in Fig. 5(a) and comprised a continuous wave (CW) laser, the EOM under evaluation fed with the corresponding bias voltage and a PIN photodetector of 10 GHz bandwidth (Discovery DSC-R402AC). The optical power at the input of the EOM was P_{IN} = 7 dBm.

Figure 5(b) shows the SFDR performance and the variation of the output optical power of the modulator (in this setup is the power arriving to the photodiode, P_{PIN}), whilst changing the modulator bias voltage. It can be observed firstly that the maximum SFDR is 0.7 dB higher in the dual-drive modulator than in a conventional modulator, achieving 40.6 dB SFDR in the optimum bias point. In addition and which is more important, the linear regime of the modulator is greatly increased using the dual-drive modulation scheme. It can be seen in Fig. 5(b) that the SFDR is in excess of 25 dB over 1.4 V range using the DD-MZ-EOM compared with a 0.5 V range in the single-MZ-EOM. This extended linear regime provides significantly more stability for radio-over-fiber systems.

#155666 - $15.00 USD
Received 3 Oct 2011; accepted 9 Oct 2011; published 22 Nov 2011
(C) 2011 OSA

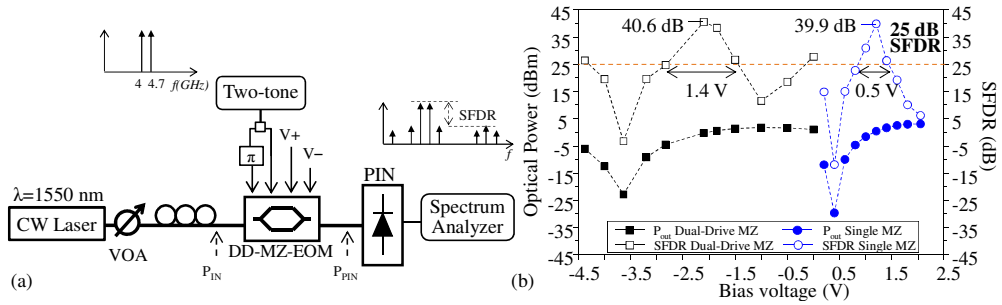

Fig. 5. (a) Experimental setup for two-tone distortion evaluation of the dual-drive modulator. (b) Output optical power and SFDR experimental results of the DD-MZ compared with a conventional single MZ.

5. Demonstration for high peak-to-average OFDM-based communication systems

To evaluate the improvement of the DD-MZ in radio-over-fiber applications, an experiment was performed based on UWB radio transmission in passive optical networks as shown in Figs. 6(a) and 6(b). An OFDM-UWB fully-compliant WiMedia channel centered on 4.488 GHz with 528 MHz bandwidth and using dual carrier modulation (DCM) at 480 Mbit/s [6] was transmitted through different fiber links. DCM MB-OFDM UWB systems have a high PAPR problem [3] which is reduced using the DD-MZ proposed scheme. Figure 6(c) shows the EVM performance of both modulators using the OFDM-UWB signal. The EVM limit according to current standards is −17 dB for UWB signals using 480 Mbit/s [6]. In Fig. 6(c) it can be observed that the dual-drive modulator performance is always better when the optical power at the photodiode is more than −10 dBm. Figure 7(a) confirms that the chirp enhances the performance when combined with fiber transmission and this improves with distance. EVM improvements of 1.9 dB and 2.2 dB over 44 km and 57 km SSMF respectively were measured (Fig. 7(a)). The DCM OFDM-UWB constellations received after different lengths are compared in Fig. 7(b). It can be observed that with DD-MZ the EVM limit is met without optical amplification even after 44 km SSMF and after 57 km the clear points of the constellation are still observable with an improvement of 2.2 dB over a single-MZ.

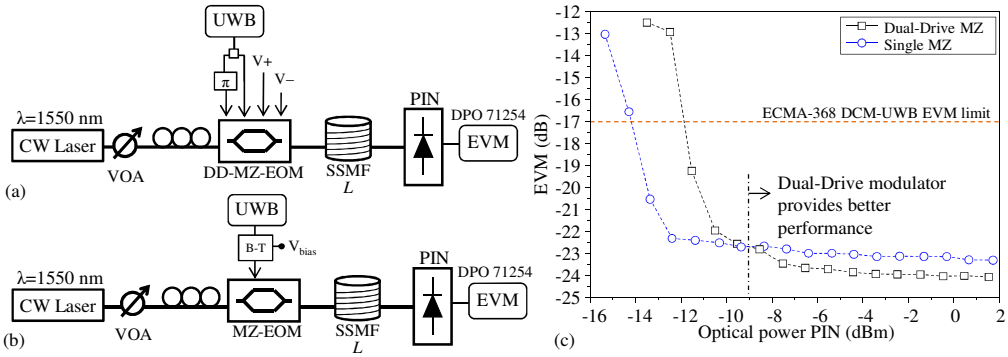

Fig. 6. Experimental setup for UWB-over-fiber transmission using: (a) the DD-MZ and (b) single MZ-EOM. (c) Measured EVM for both single and DD-MZ in back-to-back for different optical power arriving at the photodiode.

#155666 - $15.00 USD
Received 3 Oct 2011; accepted 9 Oct 2011; published 22 Nov 2011
(C) 2011 OSA

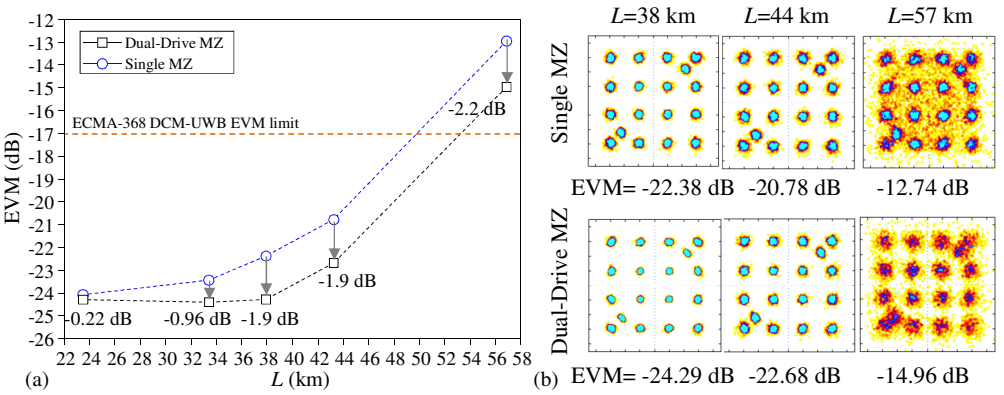

Fig. 7. (a) Measured EVM of Dual-Drive MZ compared with Single MZ after different fiber transmission lengths (*L*). EVM improvement of the DD-MZ labeled for reference. (b) DCM OFDM-UWB constellations comparison.

6. Conclusion

This paper reports the results of the dual-drive modulator designed and evaluated for enhanced linearity and chirp management. A linear regime extension with SFDR > 25 dB over 1.4 V bias range is achieved compared with the 0.5 V range of a conventional MZ-EOM, which provides enhanced linearity for radio-over-fiber transmissions. UWB transmission over PON was successfully demonstrated over 44 km SSMF with EVM < –22 dB. Additionally, chirp and PAPR control improves the UWB EVM by 2.2 dB after 57 km transmission.

Acknowledgments

This work has been partly funded by FP7 FIVER-ICT-4-249142 and UCELLS-FP7-IST-1-216785 projects. M. Morant's work is supported by Spain FPU MEC grant AP2007-01413. EUROFOS NoE is also acknowledged.